Conformation-Specific Spectroscopy of 3-Benzyl-1,5-hexadiyne

Talitha M. Selby, Aloke Das,† Tefsit Bekele,‡ Hsiupu D. Lee, and Timothy S. Zwier*

Department of Chemistry, Purdue University, West Lafayette, Indiana 47907-2084

Received: June 1, 2005; In Final Form: July 19, 2005

3-Benzyl-1,5-hexadiyne (BHD) was studied by a combination of methods, including resonance-enhanced-two-photon ionization, UV−UV hole-burning spectroscopy, resonant ion-dip infrared spectroscopy, and rotational band contour analysis. There are five conformations of BHD observed in the expansion with their $S_1 \leftarrow S_0$ origins occurring at 37520, 37565, 37599, 37605, and 37631 cm^{-1}. DFT calculations predict six low energy conformations. Conformational assignments have been made by comparison of the experimental infrared spectra in the alkyl and acetylenic CH stretch region to DFT vibrational frequency and infrared intensity calculations. Rotational band contours provided further confirmation of these assignments. The electronic origin shifts of BHD compare favorably to the electronic origin shifts of 5-phenyl-1-pentyne with the exception of one conformation. This conformation is unique in that it is the only structure with both acetylenic groups in the gauche position over the ring. This gauche−gauche conformation exhibits a perpendicular (*b*-type) transition and produces extensive vibronic coupling reminiscent of symmetric monosubstituted benzenes.

I. Introduction

Substituted benzenes play an important role in the pathways to larger PAH molecules in fuel combustion processes.[1,2] The chemical complexity of many of the substituted aromatics in fuels and fuel-rich flames opens the possibility for structural and conformational isomers. Different structural isomers can have substantially different chemical reactivity.[3] Additionally, in molecules with conformational flexibility, conformational isomerization often precedes structural isomerization by bringing the reacting segments of the molecule in close proximity where reaction can occur.

3-Benzyl-1,5-hexadiyne ($C_6H_5-CH_2-C_6H_5$) (Figure 1) is intriguing because it contains a UV "tag" attached to 1,5-hexadiyne (C_6H_6). 1,5-hexadiyne is the first minimum on the potential energy surface of the head-to-head recombination of two propargyl radicals to form benzene.[3] This C_6H_6 potential energy surface has been theoretically characterized by Miller and Klippenstein.[3] Many of the C_6H_6 structural isomers on this surface (1,5-hexadiyne, 1,2,4,5-hexatetraene, 3,4-dimethylenecyclobutene, fulvene, 1,2-hexadiene-5-yne, 2-ethynyl-1,3-butadiene) have broad UV absorptions[4−7] and are thus difficult to differentiate in the expansion with laser based techniques. On the other hand, with a UV tag, the different $C_6H_5-CH_2-C_6H_5$ structural isomers can be differentiated with isomer-specific double-resonance laser techniques. The characterization of this modified potential energy surface is one motivation for the present study.

Another goal of this study is to characterize the conformational minima of 3-benzyl-1,5-hexadiyne (BHD) as an extension to the study of the conformation-specific spectroscopy of phenylalkynes. BHD is a branched chain alkynylbenzene in which the two branches fuse together butyne and pentyne straight chains (Figure 1). The conformational spectroscopy of the two corresponding phenylalkynes, 5-phenyl-1-pentyne and 4-phenyl-1-butyne, was the subject of the preceding paper.[8] By comparison, BHD is a natural next step toward more conformationally complex phenylalkynes. In future work, we hope to use this foundation of single-conformation spectroscopy of the single and branched chain phenylalkynes to study the isomerization energetics and dynamics of this series using the newly developed method of stimulated emission pumping-population transfer spectroscopy.[9−13]

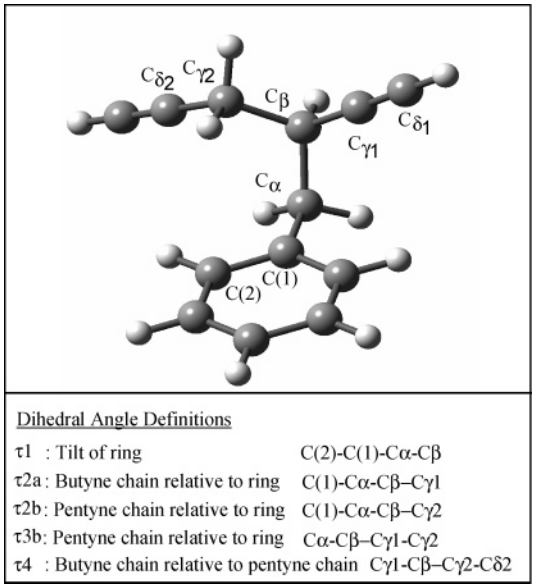

Figure 1. Picture of 3-benzyl-1,5-hexadiyne with important dihedral angles specified.

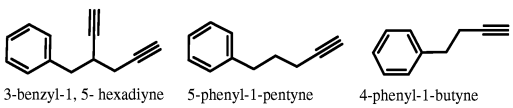

* Corresponding author. E-mail: zwier@purdue.edu. Telephone: (765) 494-5278. Fax: (765) 494-5330.

† Present address: Advanced Light Source, Lawrence Berkeley National Laboratory, Berkeley, CA 94720.

‡ Present address: Department of Chemistry, Johns Hopkins University, Baltimore, MD 21218.

10.1021/jp052923s CCC: $30.25
Published on Web 09/01/2005

The present spectroscopic studies build on earlier work on the ultraviolet spectroscopy of a series of alkyl- and alkynyl-substituted benzenes.[8,14−16] Those studies noted that those conformations in which the chain was in the gauche position relative to the ring had a $S_1 \leftarrow S_0$ origin that was red-shifted from anti conformers by about 60 cm^{-1}. In the preceding paper on 4-phenyl-1-butyne and 5-phenyl-1-pentyne,[8] the correlation between the electronic frequency shift and the conformation was developed further by viewing the effect of the chain length and position of the terminal alkynyl group. The present study of 3-benzyl-1,5-hexadiyne affords another opportunity to probe such effects in a still more complicated case in which two ethynyl groups can interact with the ring.

Finally, the rotationally resolved and partially rotationally resolved electronic spectroscopy of the above-mentioned substituted-benzenes has highlighted the unusual sensitivity of the direction of the transition dipole moment for the S_0-S_1 transition to the conformation of the substituent. While structures that are anti about the Cα−Cβ bond show nominally perpendicular (*b*-type) transitions, gauche structures produce hybrid bands (*a*-, *b*-, and *c*-type) with up to 30° swings in the direction of the TDM with conformation.[8,17] The change in the TDM direction in going from anti to gauche structures is attributed to the off-axis nature of the gauche structure which causes a mixing of the excited-state molecular orbitals to form mixed $^1L_a/^1L_b$ states.[17] CIS calculations of these systems correctly predict these results.[17] 3-benzyl-1,5-hexadiyne offers another opportunity to view the connection between TDM direction and the nature and conformation of the substituent.

II. Methods

A. Experimental Details. The procedure used to synthesize 3-benzyl-1,5-hexadiyne is provided in the Supporting Information.

The experimental apparatus and methods used for the spectroscopic studies have been described in detail elsewhere.[13,18,19] Resonance-enhanced two-photon ionization (R2PI), UV hole-burning et al. on scans, and lifetime studies were all carried out in a manner similar to that used in the preceding paper, to which the reader is referred for details.[8] A unique aspect of the present work was the use of resonant ion-dip infrared spectroscopy (RIDIRS) to record infrared spectra of single conformations of BHD. The infrared source used for RIDIR spectroscopy was a tunable Nd: YAG pumped optical parametric converter (LaserVision). To record conformation-specific infrared spectra, the UV laser (∼0.2 mJ/pulse at 20 Hz) was fixed on the $S_1 \leftarrow S_0$ origin transition of one of the conformations of interest. The infrared laser power was sufficient to remove a measurable fraction of the ground-state population when on resonance with an infrared transition (1−10 mJ/pulse at 10 Hz). The difference in ion signal created by the infrared laser was monitored using active baseline subtraction in a gated integrator.

To obtain rotational band contours, 2C-R2PI was used with an intracavity Etalon to increase the resolution of the dye laser. In this case, the resonant laser power was kept low (10−50 μJ/pulse) in order to avoid saturation effects, and the ionization laser power was high (1.0 mJ/pulse, $\lambda \geq 270$ nm) to increase the signal. 2C-R2PI was also used to obtain the excited-state lifetime where the ion signal was monitored as a function of delay time between the resonant and ionization lasers. The BHD sample was heated to ∼50 °C and entrained in the expansion with either 5 bar pure helium or 4 bar 70% Ne/30% He mixture at 20 Hz with a pulsed valve (R. M. Jordan Co.).

B. Computational Details. Molecular mechanics (MM) methods with the Amber force field were used for conformational searching of starting structures for quantum mechanical calculations. Density functional theory (DFT) calculations with a Becke3LYP[20,21] functional and a 6-31+G*[22] basis set were used to determine more accurate structures and energies. True minima were verified by the lack of imaginary frequencies. Second-order Moller−Plesset perturbation (MP2) with cc-pVDZ[23] basis set optimizations and single point energy calculations with the aug-cc-pVDZ basis set[23,24] were also performed on DFT/6-31+G* and MP2/cc-pVDZ optimized structures. Configuration interaction singles (CIS)[25] and Hartree−Fock (HF) calculations with a 6-31G basis set were performed on selected minima for simulations of rotational band contours in which the ground and excited-state rotational constants and transition dipole moments are used as parameters. MM calculations were performed using MacroModel software.[26] DFT, MP2, HF, and CIS computations were carried out using Gaussian 98.[27] Rotational band contour simulations were performed using the JB95 software.[28]

III. Results and Analysis

A. Computational Details. MM calculations resulted in 16 minima for BHD within 21 kJ/mol of the global minimum. These structures were used as the starting structures in DFT optimizations. From these DFT optimizations, 11 unique structures resulted with six structures within 9 kJ/mol of the global minimum. Figure 2 presents these six lowest energy structures.

The six lowest energy structures can be distinguished from one another by the orientation of each chain with respect to the ring and the orientation of the two chains with respect to each other. The defining angles used to distinguish different conformations are labeled in Figure 1 and used in the naming scheme shown in Figure 2. The dihedral angle definitions are consistent with those in the preceding paper for 4-phenyl-1-butyne and 5-phenyl-1-pentyne. For example, the first letter describes the butyne chain relative to the ring (a = anti and g = gauche) and is defined by the dihedral angle, τ2a, as shown in Figure 1 (anti structures have τ2a ≈±180 and gauche structures have τ2a ≈ ±60). Similarly, the second and third letters in the name describe the conformation of the pentyne chain relative to the ring (aa, ag, ga, gg) and they differ in the dihedral angles τ2b and τ3b. The last letter describes the orientation of the two chains relative to each other and is defined by the dihedral angle, τ4, as shown in Figure 1 (anti structures have τ4 ≈±180 and gauche structures have τ4 ≈ ±60). Table 1 summarizes the DFT results for the key structural parameters and rotational constants of the lowest energy structures of BHD.

The zero point corrected DFT relative energies of each structure are shown in Figure 2, and Table 2 summarizes the relative energies calculated at DFT and MP2 levels of theory (with several different basis sets), both with and without ZPE corrections. Much as was found for PB and PP in the preceding paper, the MP2 calculations favor structures with the pentyne chain in the gg position and reorders the energies of the low energy structures. This method also spreads the energies of the conformers over a wider range. The similarities in the single point MP2/aug-cc-pVDZ calculations on both the DFT and MP2 optimized structures confirms the difference in the energy orderings is due to the level of theory and not the basis sets used.

The lowest energy BHD structure (according to DFT), g(ag)a, has the pentyne chain in the anti position with the butyne chain

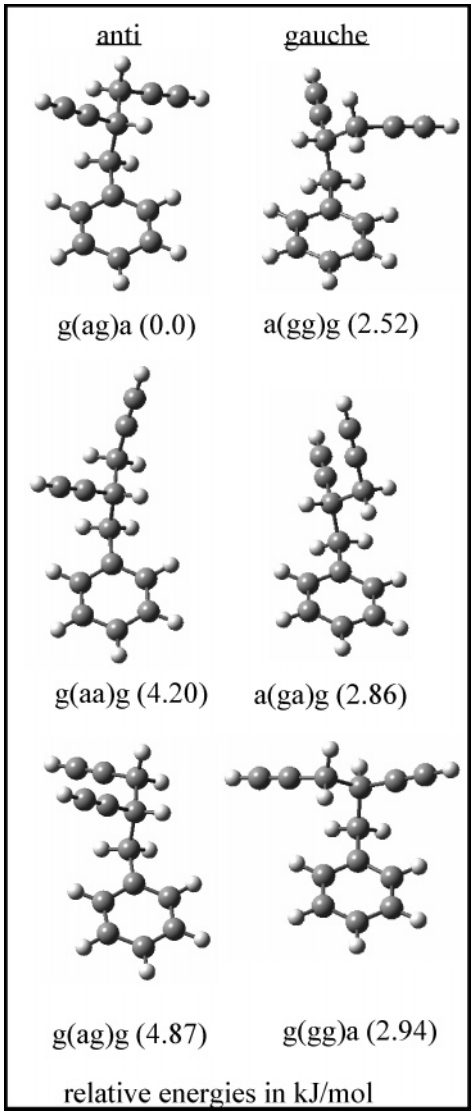

Figure 2. Pictorial summary of the six lowest energy structures of BHD. The six species are separated into two groups which differ in the position of the pentyne chain's gamma methylene group relative to the ring (anti on left and gauche on right). The relative energies of each structure at DFT (B3LYP/6-31+G*) level of theory are given in parentheses. The naming scheme is described in the text.

in the gauche position and both chains in the anti position with respect to each other (Figure 2). The next three low energy structures (a(gg)g, g(gg)a, and a(ga)g) each have the pentyne chain in the gauche position (Figure 2). The g(gg)a structure also has its butyne chain in the gauche position (Figure 2). It is the only structure that has both chains in the gauche configuration over the ring (Figure 2). The 1,5-hexadiyne subunit in g(gg)a takes up an anti configuration (Figure 2).

B. R2PI and UVHB Spectra. Figure 3 presents the overview 1C-R2PI spectrum of BHD in the low-energy region of the $S_1 \leftarrow S_0$ transition. The spectrum bears a close resemblance to the excitation spectra of the alkylbenzenes recorded by Smalley and co-workers[16] and the phenylalkynes studied in our laboratory.[8] Like all substituted benzenes, most of the Franck−Condon (FC) activity is in the ring modes. The positions of the $S_1 \leftarrow S_0$ origin and several strong vibronic transitions (in Wilson notation) of the anti conformer of *n*-propylbenzene are shown above the BHD spectrum for comparison.[16]

Parts a and b of Figure 4 present the 1C-R2PI spectra expanded in the origin region (Figure 4a) and at an intermediate scale that extends through the $6b^1_0$ region (Figure 4b). The UHVB spectra of conformers BHD(A−C) (Figure 4c−e) are shown below the R2PI spectrum (Figure 4b). Most transitions in the R2PI spectrum are accounted for by conformers BHD-(A−C). Conformer BHD(E) was identified through the transitions not accounted for by the UVHB spectra of conformers BHD(A−C). The UVHB spectra of BHD(E) (not shown) were obtained only over regions of unidentified transitions. Three transitions of BHD(E) were found. The UVHB spectra of BHD-(E) were not taken over the entire region because the noise from the large signal of the other conformers was of the same magnitude as the BHD(E) signal. Another conformation BHD-(D) only has enough population to detect the origin transition. It did not hole-burn out with any other conformation. The 0^0_0 and $6b^1_0$ transitions are labeled for each conformation in Figure 4.

The two transitions marked with asterisks in Figure 4b are due to an impurity of the same mass in the sample. It was determined that these transitions were due to an impurity based on the fact that R2PI spectra of BHD were taken with two different samples, and these transitions were not present in both samples. In the sample where they were present, these transitions did not decrease in relative intensity after changing the nozzle conditions. Moreover, no evidence of dimers or clusters was found. Interestingly, the excited-state lifetime of the impurity (∼20 ns) is much shorter than the lifetime of BHD (∼80 ns). Given that 1,5-hexadiyne and benzyl chloride are the starting materials in the synthesis of 3-benzyl-1,5-hexadiyne, it is likely that the impurity is due to an end-on addition of 1,5-hexadiyne to benzyl chloride resulting in a straight chain isomer (see Supporting Information); however, this has not been confirmed.

All transitions in the R2PI spectrum (Figure 4a,b) are accounted for by the five conformations of BHD and the impurity. The assignment of these five species as conformers of BHD was confirmed by the unique infrared spectra recorded for each of them when monitoring the origin transitions of conformations BHD(A−E) (see below).

The S_0-S_1 origin transitions of the BHD conformers E, A, D, B, and C occur at 37520, 37565, 37599, 37605, and 37631 cm^{-1}, respectively (Figure 4). The $6b^1_0$ transition occurs at 530/533, 533, 535, and 531 cm^{-1} above the origin in BHD(A−C, and E), respectively (Figure 4). As anticipated, there is not much difference in the observed frequencies of this mode between the different conformations. These conformers do show small differences in the frequencies of the chain-ring torsion which occur at 33, 26, 30, and 31 cm^{-1} in BHD(A−C, and E), respectively (Figure 4). Other low-frequency modes also show subtle differences in frequency between different conformations; however, assignments to the other modes must await dispersed fluorescence studies. The most notable difference between the UVHB spectra recorded is the much greater degree of vibronic coupling observed in BHD(C) (Figure 4e) than in the other conformers. BHD(C) has five transitions between 370 and 540 cm^{-1} above the origin with greater intensity than the origin band (Figure 4e). Of these transitions, $6b^1_0$ has the greatest intensity. Rotational band contours of the 0^0_0 and $6b^1_0$ (see below) transitions confirm that the $6b^1_0$ is vibronically induced.

Lifetimes of several vibronic transitions of the three main isomers of BHD were taken. All transitions in the first 1500 cm^{-1} had lifetimes of 80 ± 5 ns, independent of conformation. At energies between 1500 and 2500 cm^{-1} above the origin the lifetime slowly dropped off from ∼75 to ∼55 ns.

C. RIDIR Spectra in the CH Stretch Region. 1. Overview of the CH Stretch Region. Parts a−e of Figure 5 present

TABLE 1: Selected Structural Parameters for the Six Lowest Energy Minima of BHD at DFT (B3LYP/6-31+G*) Level of Theory

	parameter								
							rotational constants		
structure	τ1, deg	τ2a, deg	τ2b, deg	τ3b, deg	τ4, deg	C(1)−Cα, Å	A'', MHz	B'', MHz	C'', MHz
g(ag)a	99.49	−66.01	170.99	−63.42	172.06	1.514	1306	475	378
a(gg)g	78.86	−171.42	62.48	60.45	−65.24	1.515	1441	487	396
g(gg)a	91.58	63.81	−61.54	−61.39	−171.75	1.515	1065	621	439
a(ga)g	72.88	−171.75	64.06	−172.42	64.17	1.515	1406	429	379
g(ag)g	98.32	−64.60	169.49	59.71	−66.87	1.514	1671	419	395
g(aa)g	98.80	−64.15	171.83	−171.87	63.73	1.514	1845	390	360

TABLE 2: Relative Energies (kJ/mol) of Selected Conformational Minima of BHD

level of theory(basis set) [single point//optimized structure]	E_{rel}(a(gg)g)[b]	E_{rel}(g(gg)a)[b]	E_{rel}(a(ga)g)[b]	E_{rel}(g(ag)g)[b]	E_{rel}(g(aa)g)[b]
B3LYP(6-31+G*)//B3LYP(6-31+G*)	1.76	1.97	2.73	4.79	4.58
B3LYP(6-31+G*)//B3LYP(6-31+G*) + ZPE[a]	2.52	2.94	2.86	4.87	4.20
MP2(cc-pVDZ)//MP2(cc-pVDZ)	−3.23	−4.75	2.23	1.85	4.62
MP2(cc-pVDZ)//MP2(cc-pVDZ) + ZPE[a]	−2.48	−3.74	2.35	1.89	4.24
MP2(aug-cc-pVDZ)//B3LYP(6-31+G*)+ ZPE[a]	−2.02	−3.78	2.31	4.41	5.29
MP2(aug-cc-pVDZ)//MP2(cc-pVDZ) + ZPE[a]	−3.53	−5.80	2.44	3.53	5.17

[a] Zero-point energy contributions are determined at the Becke3LYP/6-31+G* level of theory. [b] Energy relative to g(ag)a in kJ/mol.

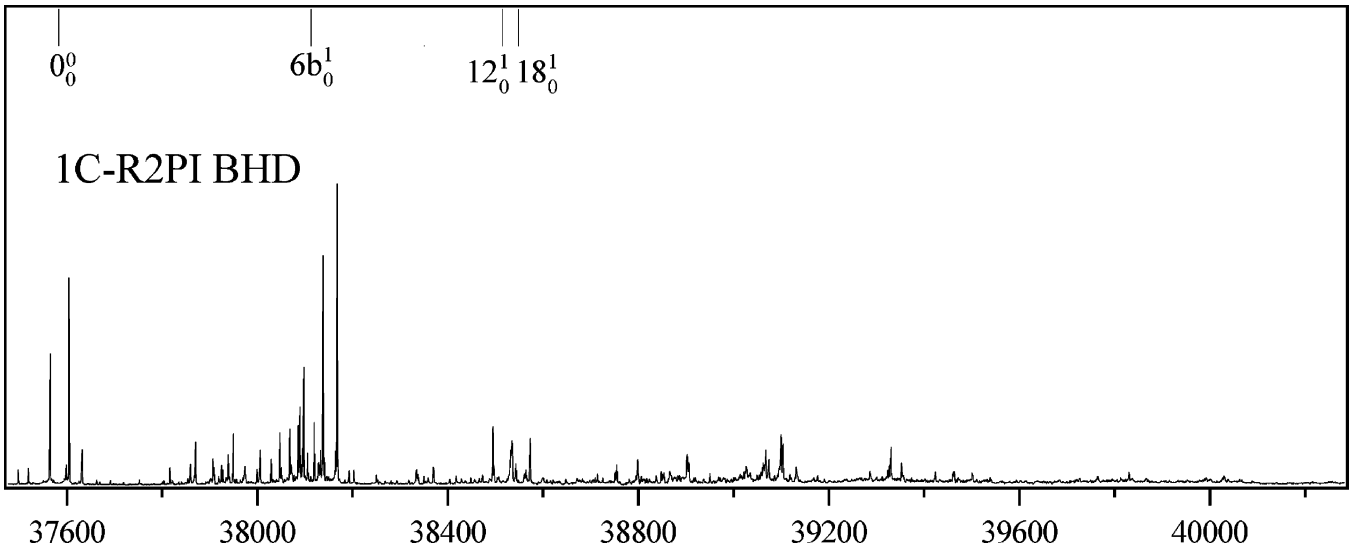

Figure 3. Overview 1C-R2PI spectrum of 3-benzyl-1,5-hexadiyne with the anti-propylbenzene[16] origin transition and selected ring modes (Wilson notation) shown for reference above the BHD R2PI spectrum.

overviews of the ground-state RIDIR spectra in the CH stretch region for 3-benzyl-1,5-hexadiyne conformers BHD(A−E), respectively. These spectra span the alkyl C−H stretch region (2890−2990 cm^{-1}), aromatic C−H stretch region (3000−3150 cm^{-1}), and acetylenic C−H stretch region (3300−3360 cm^{-1}). The aromatic CH stretch region does not show any recognizable conformer specificity, and will not be discussed further. In the acetylenic and alkyl CH stretch regions there are differences in the frequencies and intensities between different conformations. To guide the reader through these differences, expanded regions of the RIDIR spectra are shown in Figures 6−8 alongside DFT (B3LYP/6-31+G*) calculated frequencies and intensities. The reader is encouraged to refer back to Figure 5 for the relative intensities of transitions observed in different regions.

2. Acetylenic CH Stretch Region. The left-hand side of Figure 6 presents expanded views of the ground-state RIDIR spectra in the acetylenic CH stretch region of BHD conformers (a) BHD(E), (b) BHD(A), (c) BHD(D), (d) BHD(B), and (e) BHD(C). These spectra were taken at low infrared power (∼1.0 mJ/pulse) to reduce power broadening. Small but systematic shifts in the frequency, over-all width, and shape of the bands are observed from one conformation to the next. Since BHD contains two acetylenic CH groups, we anticipate two acetylenic CH stretch fundamentals for each isomer. These variations from one conformer to the next reflect the relative orientation and degree of coupling between the two acetylenic CH groups.

Harmonic frequencies of the acetylenic CH stretches, calculated using DFT (B3LYP/6-31+G*) with a 0.9565 scale factor, are also shown in Figure 6 (right). Both the experimental and simulated spectra are arranged from highest frequency (top) to lowest (bottom). In BHD, the two acetylenic groups are part of a 1,5-hexadiyne subunit that place the two acetylenic groups either gauche or anti with respect to one another (Figures 1 and 2). The ordering of the spectra from high to low-frequency places the four lowest energy gauche hexadiyne structures on the top (Figure 6a−d, right) and the two low-energy anti conformers on the bottom (Figure 6e,f right). It is interesting that the ordering of RIDIR spectra from high (BHD(E)) to low frequency (BHD(C)) is the exact reverse ordering of the electronic origin shifts.

The gauche or anti configuration for the 1,5-hexadiyne subunit also affects the relative intensities and splittings of the bands. In particular, conformers with the acetylenic groups anti with respect to one another have very little intensity in the symmetric

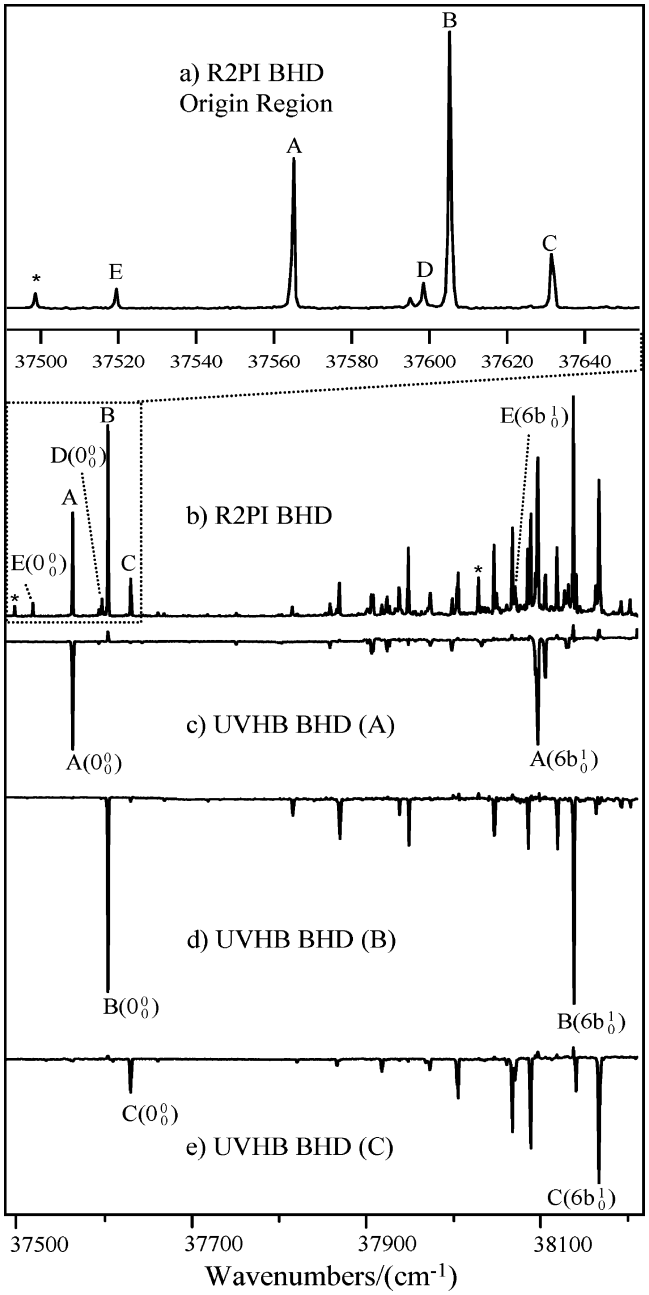

Figure 4. 1CR2PI spectra of 3-benzyl-1,5-hexadiyne (a) expanded in the origin region and (b) out through the $6b^1_0$ region, and UVHB spectra of conformers (c) BHD(A), (d) BHD(B), and (e) BHD(C). Conformer BHD(E) was identified through the transitions not accounted for by the UVHB spectra of conformers BHD(A−C). The UVHB spectra of BHD(E) (not shown) were obtained only over regions of unidentified transitions. Three transitions of BHD(E) were found. Another conformation BHD(D) only has enough population to detect the origin transition. It did not hole-burn out with any other conformation. Two transitions marked with asterisks are due to an impurity of the same mass in the sample. The 0^0_0 and $6b^1_0$ transitions are labeled for each conformation.

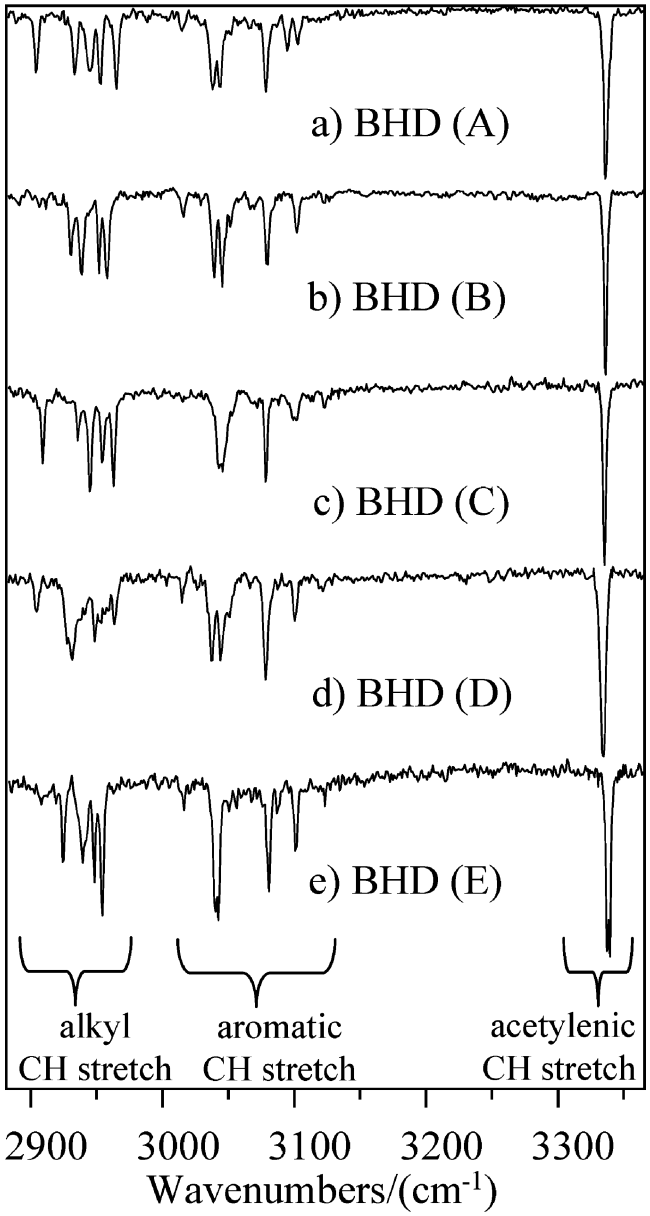

Figure 5. (a−e) Overview of the ground-state RIDIR spectra in the CH stretch region of BHD(A−E), respectively. The different CH stretch regions are labeled for reader reference.

CH stretch fundamental because the oscillating dipoles of the two CH groups almost cancel. Unfortunately, the small frequency shifts prevent resolution of the two fundamentals. Instead, the small intensity in the symmetric stretch should show up indirectly in the experimental spectra as particularly narrow widths for the acetylenic band due to the fact that only one transition contributes to it. As just predicted, the two structures with the smallest experimental width, BHD(B) and BHD(C), are those that, according to the frequency shift, are the two *anti*-hexadiyne structures, g(ag)a and g(gg)a, respectively. Thus, based both on the width and frequency shifts we tentatively assign BHD(B) and BHD(C) to the "*anti*"-hexadiyne structures g(ag)a and g(gg)a. Furthermore, based on the frequency, we would tend to favor an assignment of BHD(B) to g(ag)a and BHD(C) to g(gg)a, respectively.

In gauche structures, both acetylenic CH stretch fundamentals carry appreciable intensity. When the two bands are unresolved, the magnitude of the splitting is reflected in the breadth of the observed band.

The tentative assignment of BHD(B) and BHD(C) to anti hexadiyne structures leaves BHD(A), BHD(E), and BHD(D) to gauche structures. Of the experimental spectra, only BHD(E) shows two resolved bands, indicating that it has the largest splitting of the five. This would favor an assignment of BHD(E) to either a(ga)g or g(aa)g, consistent with the fact that these two conformers have the most blue-shifted of the computed bands. Arguments based on the alkyl CH stretch fundamentals favor only one of these conformers being present in the expansion. By comparing the calculated splittings (Figure 6,

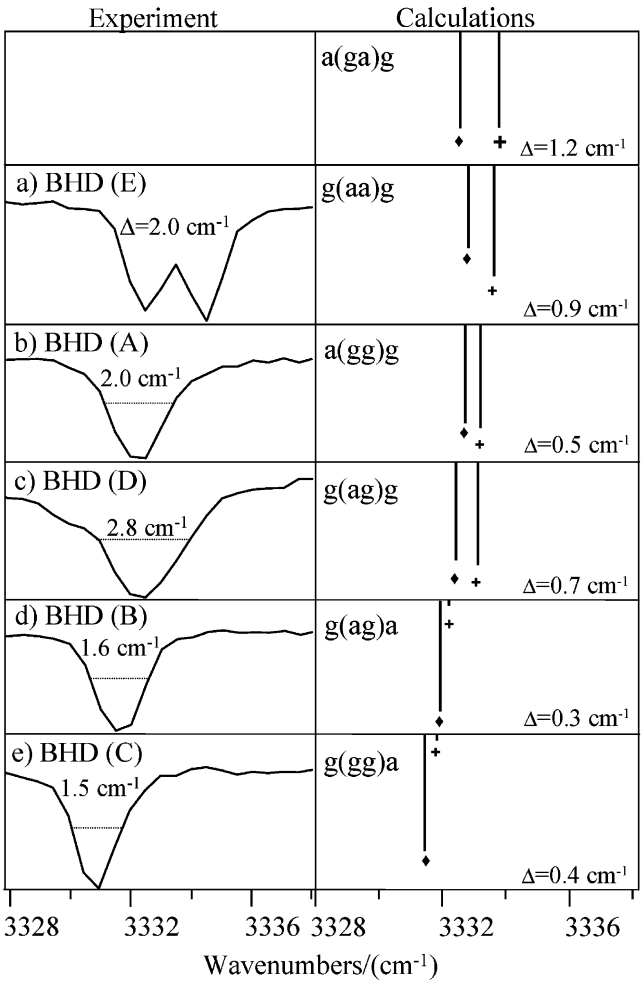

Figure 6. Left: Expanded views of the ground-state RIDIR spectra in the acetylenic CH stretch region of BHD conformers (a) BHD(E), (b) BHD(A), (c) BHD(D), (d) BHD(B), and (e) BHD(C). These spectra were taken at low infrared power (~1.0 mJ/pulse). Right: Calculated DFT (B3YYP/6-31+G*) harmonic frequencies of the acetylenic CH stretches scaled by 0.9565. Both the experimental and simulated spectra are arranged from most blue-shifted (top) to red-shifted (bottom). The experimental spectra have the fwhm for each conformer labeled with the exception of conformer BHD(E) which has the peak splitting labeled. The simulated spectra have the antisymmetric stretches marked with a diamond (♦) and the symmetric stretches marked by a cross (+). The calculated splitting between the antisymmetric and symmetric stretches is also labeled in the bottom right-hand corner for each structure.

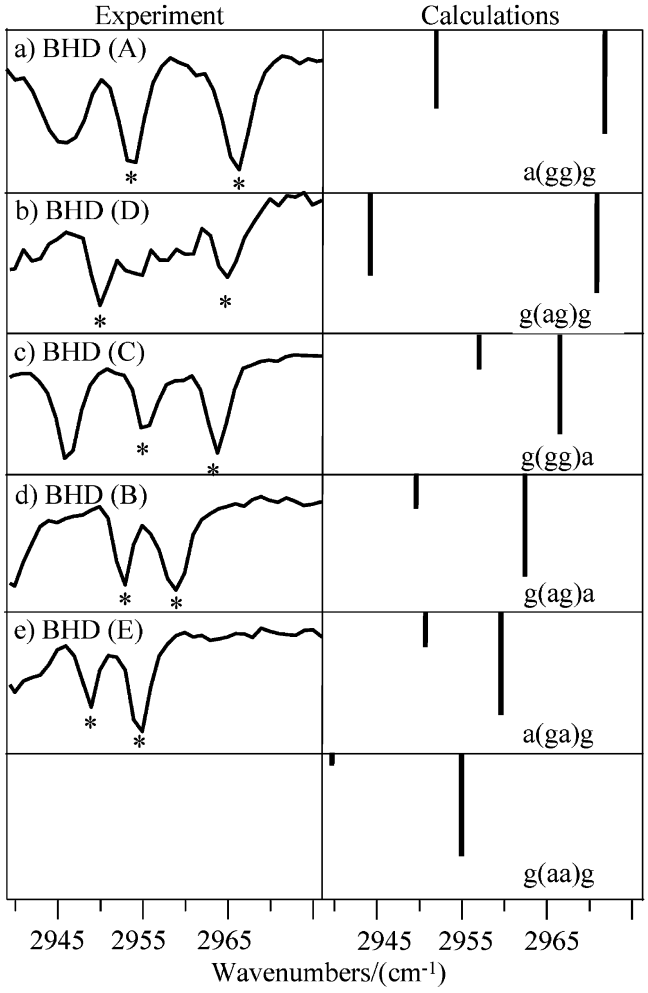

Figure 7. Left: Expanded views of the ground-state RIDIR spectra in the antisymmetric (AS) CH stretch region of BHD conformers (a) BHD(A), (b) BHD(D), (c) BHD(C), (d) BHD(B), and (e) BHD(E). Right: The calculated DFT (B3YYP/6-31+G*) harmonic frequencies of the AS alkyl CH stretches scaled by 0.9565. Both the experimental and simulated spectra are arranged from most blue-shifted (top) to red-shifted (bottom) of the $C_\alpha H$ AS stretch. The AS CH stretches are labeled by an asterisk (∗) in the experimental RIDIR spectra.

right) of the remaining gauche structures to the experimental width (left) of the remaining two conformers, we see that BHD-(A) has the smallest width in the RIDIR spectra of the two, and a(gg)g has the smallest splitting of the remaining gauche structures. This would leave BHD(D) to the g(ag)g structure, consistent with its intermediate frequency and width. Thus, based on the acetylenic CH stretch region, we tentatively assign, BHD(A) to a(gg)g, BHD(D) to g(ag)g, and BHD(E) to either a(ga)g or g(aa)g.

3. Alkyl CH Stretch Region. a. The Antisymmetric Stretches. The left side of Figure 7 presents expanded views of the ground-state RIDIR spectra in the antisymmetric (AS) CH stretch region of BHD conformers (a) BHD(A), (b) BHD-(D), (c) BHD(C), (d) BHD(B), and (e) BHD(E). The calculated harmonic frequencies of the AS alkyl CH stretches are also shown in Figure 7 (right). As before, both the experimental and calculated spectra are arranged from highest (top) to lowest frequency (bottom) of the $C_\alpha H$ AS stretch, using the highest-frequency AS stretch fundamental as reference. In arranging the experimental and calculated structures in this manner, it is easy to see that the tentative assignments from the acetylenic CH stretch obtain additional support from the alkyl CH stretch region. For example, BHD(A) possesses the highest frequency band in the experimental RIDIR spectra, while a(gg)g is predicted to be highest in frequency by calculation (Figure 7a). Likewise, BHD(E) is lowest in frequency in the experimental spectra, while a(ga)g and g(aa)g are the furthest red-shifted in the calculated spectra (Figure 7e).

The observed splittings between the $C_\alpha H$ and $C_{\gamma 2} H$ AS stretches are also qualitatively consistent with the preliminary assignments. For example, BHD(D) and BHD(A) have relatively large splittings, consistent with the large calculated splittings for g(ag)g and a(gg)g. Similarly, BHD(C), BHD(B), and BHD-(E) have relatively small splittings observed experimentally in the same way as the calculated spectra of g(gg)a, g(ag)a, a(ga)g, and g(aa)g. As in the acetylenic CH stretch region, the RIDIR spectrum of BHD(E) in the AS alkyl CH region is close to the calculated spectra of both a(ga)g and g(aa)g. However, the splittings and relative intensities observed in the spectrum of BHD(E) match those in a(ga)g more closely than g(aa)g.

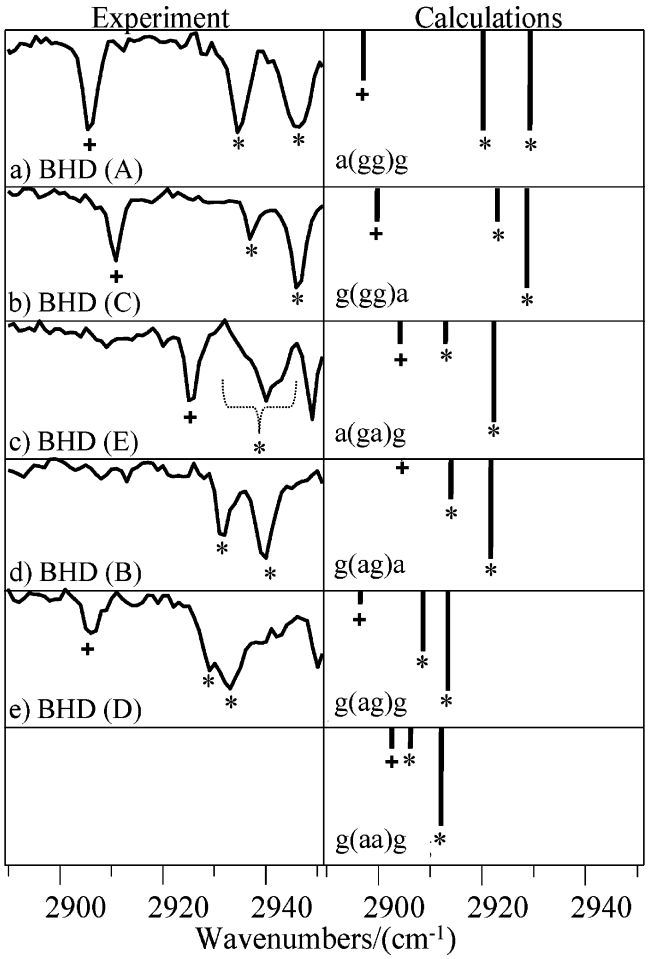

Figure 8. Left: Expanded views of the ground-state RIDIR spectra in the alkyl symmetric and C_β CH stretch region of BHD conformers (a) BHD(A), (b) BHD(C), (c) BHD(E), (d) BHD(B), and (e) BHD(D). Right: Calculated DFT (B3YYP/6-31+G*) harmonic frequencies scaled by 0.9565. Both the experimental and simulated spectra are arranged from most blue-shifted (top) to red-shifted (bottom) of the $C_\alpha H$ symmetric stretch. The symmetric stretches are labeled by an asterisk (*) and the C_β stretch is labeled with a cross (+)

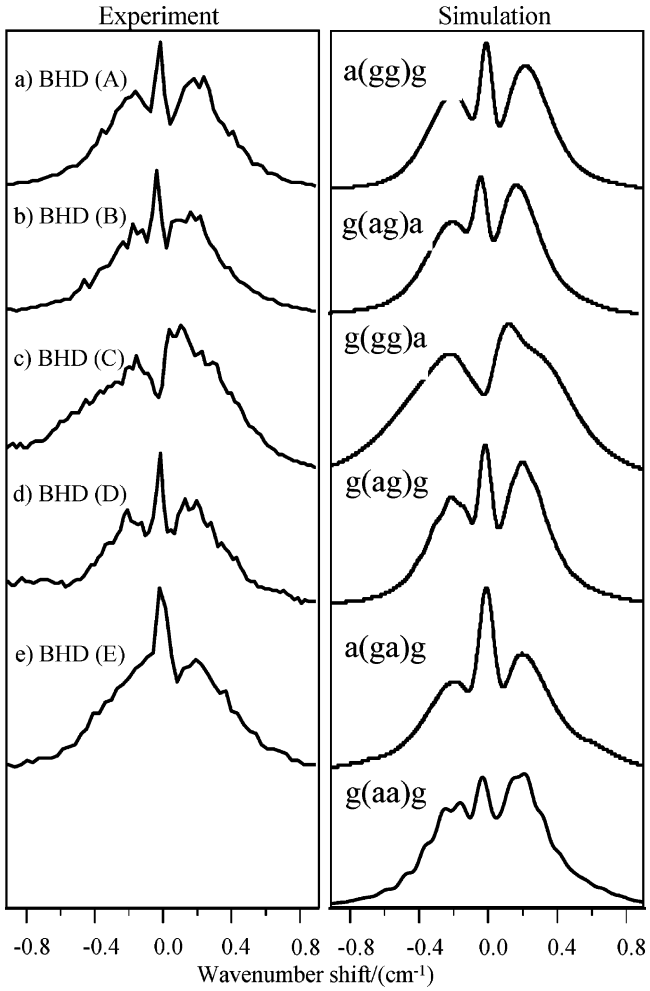

Figure 9. Left: rotational band contour spectra of the origin bands of BHD conformers (a−e) BHD(A−E). Right: Simulated band contours using the ab initio predictions for the ground and excited state rotational constants and transition dipole moments at HF(6-31G) and CIS(6-31G) levels of theory, respectively (Table 3). Rotational temperatures and the experimental resolution used in the simulations are also given in Table 3.

b. The C_β and Symmetric Stretches. Further support for the assignments are found from the alkyl symmetric stretch and C_β CH stretch fundamental transitions. Figure 8 (left) presents expanded views of the ground-state RIDIR spectra in this region for BHD conformers a) BHD(A), (b) BHD(C), (c) BHD(E), (d) BHD(B), and (e) BHD(D). The calculated DFT (B3YYP/6-31+G*) harmonic frequencies of the alkyl symmetric and C_β CH stretches scaled by 0.9565 are also shown in Figure 8 (right). As before, both the experimental and simulated spectra are arranged from most blue-shifted (top) to red-shifted (bottom), this time using the $C_\alpha H$ symmetric stretch as reference point.

In arranging the experimental and calculated structures by the shift of the $C_\alpha H$ symmetric stretch, we see that BHD(A) is the most blue-shifted in the experimental RIDIR spectra, while a(gg)g is the predicted to be the furthest blue shifted in the calculated spectra. Likewise, BHD(D) is the most red-shifted in the experimental spectra, and g(ag)g and g(aa)g are the furthest red-shifted in the calculated spectra. This arrangement also supports the assignment of BHD(E) to a(ga)g.

The relative splittings of the two symmetric stretches are also qualitatively consistent with previous assignments. For example, BHD(A) has two relatively strong symmetric stretches with a relatively large splitting which is consistent with calculations for a(gg)g. BHD(B) and BHD(C) both have a strong $C_\alpha H$ and weaker $C_{\gamma 2}H$ symmetric stretches consistent with the calculations for g(ag)a and g(gg)a. BHD(D) has two closely spaced and about equally intense symmetric CH stretches that are just barely resolved, consistent with the calculated transitions for g(ag)g.

The relative intensity and position of the C_β stretch is also qualitatively consistent with previous assignments. For example, BHD(A), BHD(C), and BHD(D) all have relatively strong C_β stretches that are shifted far to the red, consistent with the calculations for a(gg)g, g(gg)a, and g(ag)g. BHD(B) is missing the C_β stretch consistent with calculations for g(ag)a. BHD(E) also has a strong C_β stretch that is further blue-shifted than in the other conformers, consistent with its assignment as a(ga)g.

C. Rotational Band Contours. Rotational band contours were obtained to provide further support to the assignments made from the infrared analysis. Parts a−e of Figure 9 present (left) the rotational band contour spectra of the origin bands of BHD conformers BHD(A−E), respectively, and (right) simulations from ab initio calculations. Unlike the study of 4-phenyl-1-butyne and 5-phenyl-1-pentyne, the larger size and "doubled armed" nature of the side chain in BHD leads to less well resolved band contours that are less diagnostic of the conformation. As a result, the simulations on the right-hand side of Figure 9 are not fits but rather predictions made using the rotational

TABLE 3: Ground and Excited State Rotational Parameters for Selected Minima of BHD at HF(6-31G) and CIS(6-31G) Levels of Theory, Respectively, and Rotational Temperatures and Resolutions Used in Simulated Band Contours

	parameter								
	ground state			excited state			simulation		
	A'', MHz	B'', MHz	C'', MHz	ΔA, MHz	ΔB, MHz	ΔC, MHz	μ_a^2: μ_b^2: μ_c^2	T, K	fwhm, cm^{-1}
g(ag)a	1314	482	381	-29	-3	-3	45:37:18	1.3	0.08
a(gg)g	1466	490	400	-19	-3	-1	59:30:11	1.5	0.08
g(gg)a	1071	630	443	-11	-7	-5	10:84:6	2.3	0.10
a(ga)g	1436	429	381	-24	-1	0	37:0:63	1.5	0.09
g(ag)g	1700	424	398	-23	-4	-1	62:22:16	1.5	0.07
g(aa)g	1865	395	363	-33	-3	-1	42:32:26	1.5	0.08

constants and S_0-S_1 transition moment direction from HF(6-31G) and CIS(6-31G) calculations. There is substantial precedence for the accuracy of calculations at this level of theory in predicting transition moment directions in substituted benzenes, including PB and PP from the preceding paper.[8,14] The rotational parameters used in the simulation are given in Table 3. All bands were simulated with rotational temperatures between 1.3 and 2.3 K and resolutions between 0.07 and 0.1 cm^{-1}. Only the resolution and rotational temperatures were adjusted during the simulation to match the corresponding experimental contour.

The experimental contours of every conformer except BHD-(C) and have strong Q-branches and mixed type transitions (Figure 9 and Table 3). Of the simulated and experimental contours with Q-branches, a(ga)g and BHD(E) have the strongest Q-branches relative to the P and R branches. This similarity supports our previous assignment of BHD(E) to a(ga)g. On the contrary, the simulation of g(aa)g has a very weak Q-branch relative to the P and R branches and is the most dissimilar to the experimental band contours. This dissimilarity is also consistent with our conclusion that g(aa)g is not one of the conformers observed in the expansion. BHD(C) bears a close resemblance to the simulation of the g(gg)a structure and confirms our previous assignments of BHD(C) to g(gg)a. The transition dipole moment of BHD(C) lies along the *b*-inertial axis, perpendicular to the axis on which the substituent lies, similar to other symmetric monosubstituted benzenes.

Given that BHD(C) shows evidence of strong vibronic coupling in the excitation spectrum, the band contour of the $6b^1_0$ transition was also recorded. Figure 10 presents the experimental rotational band contours of BHD(C)'s $6b^1_0$ transition (Figure 10c), and the 0^0_0 transition (Figure 10a) is shown for comparison. The simulated contours are shown below the corresponding experimental contours (Figure 10 b and d). In both simulated spectra, a rotational temperature of 2.3 K and resolution of 0.10 cm^{-1} were used. Both simulations use the same rotational constants from HF(6-31G) and CIS(6-31G) calculations for the ground and excited states, respectively. (Table 3). The TDM used in the simulation of the $6b^1_0$ transition was obtained from the CIS calculated TDM for the $S_2 \leftarrow S_0$ transition (μ_a^2: μ_b^2: μ_c = 88:11:1).

The rotational contour of the $6b^1_0$ transition of BHD(C) has a strong Q-branch reminiscent of a parallel transition (*a*-type); where as the 0^0_0 transition is a perpendicular transition (*b*-type). This finding supports our conclusion that the $6b^1_0$ transition gains intensity via vibronic coupling with the S_2 state.

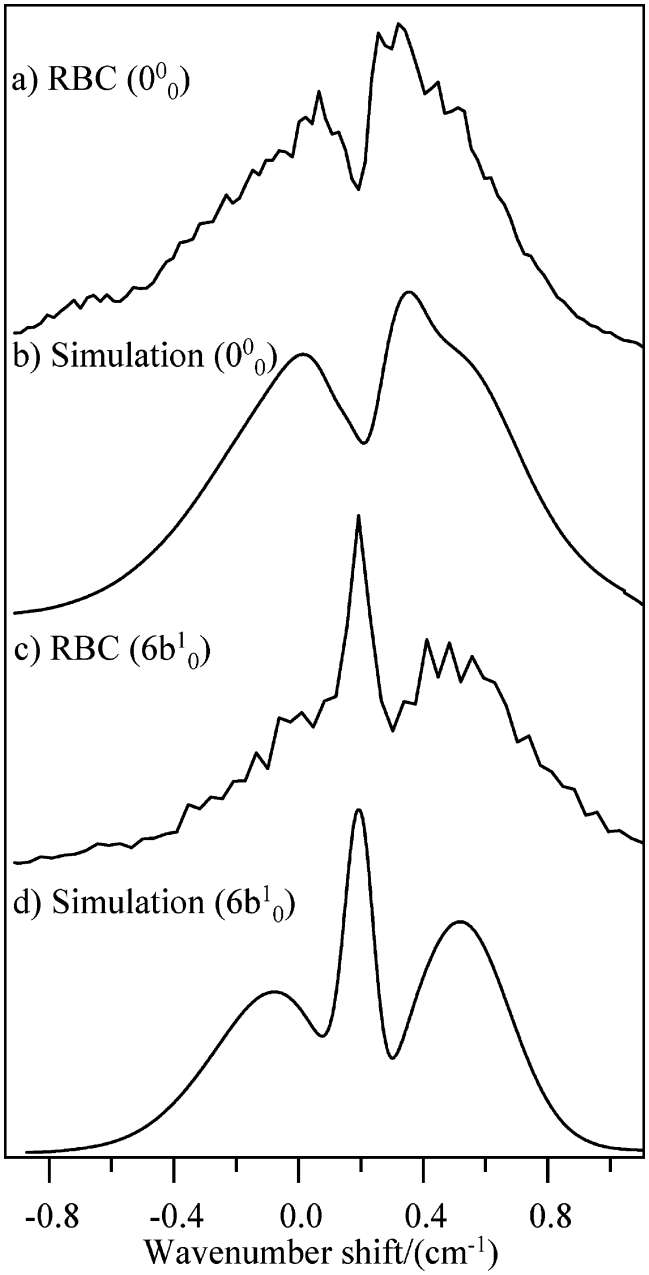

Figure 10. Rotational band contour spectra of BHD(C) of the (a) 0^0_0 and (c) $6b^1_0$ transitions and simulated contours of the (b) 0^0_0 and (d) $6b^1_0$ transitions. Simulated band contours from ab initio results of the ground and excited state rotational constants and transition dipole moments at HF(6-31G) and CIS(6-31G) levels of theory, respectively (Table 3). For simulation of the $6b^1_0$ transition, the TDM, μ_a^2: μ_b^2: μ_c (=88:11:1), of the $S_2 \leftarrow S_0$ transition was used. A 2.3 K rotational temperature and 0.1 cm^{-1} resolution were used in both simulations.

V. Discussion and Conclusions

A combination of supersonic expansion cooling and laser-based double resonance spectroscopy have been used to record isomer-specific ultraviolet and infrared spectra of five conformational isomers of 3-benzyl-1,5-hexadiyne. Ultraviolet hole-burning spectroscopy determined that five of the six calculated low energy structures of 3-benzyl-1,5-hexadiyne are present in the expansion. The infrared studies also provided unique spectral signatures of the different conformers and proved to be the most

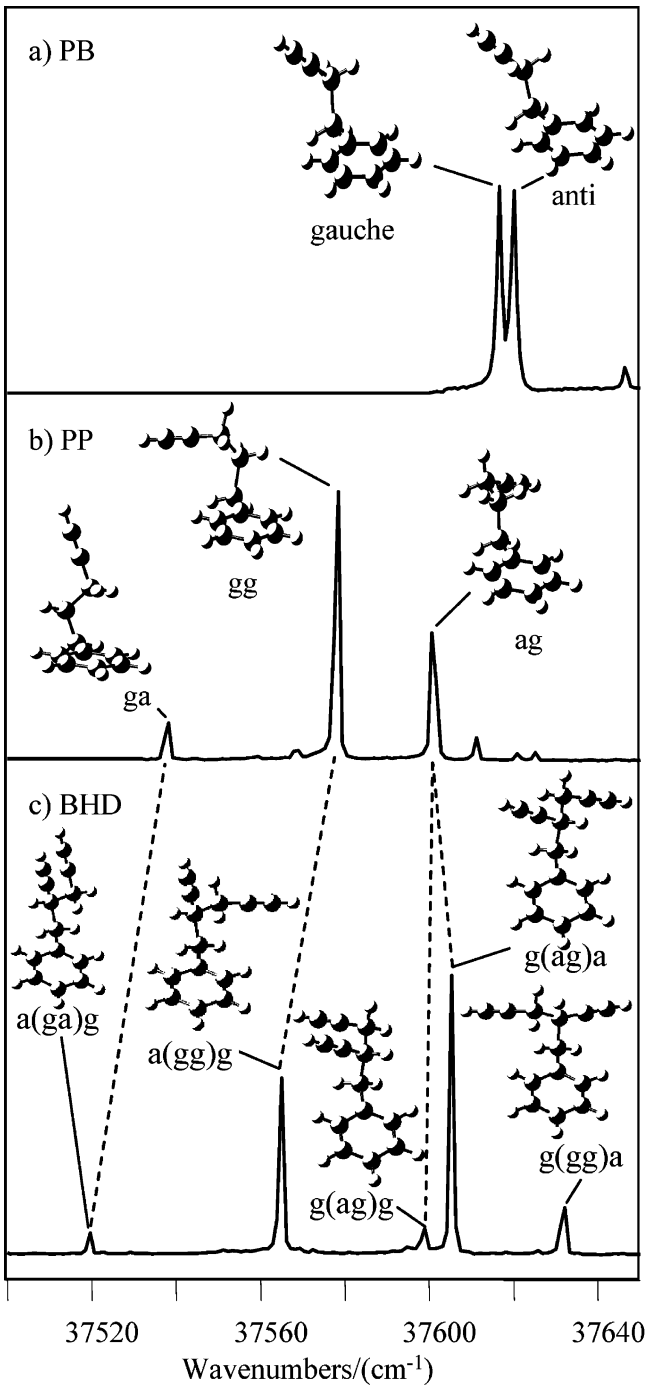

Figure 11. Summary of (c) BHD assignments with the assigned structures of (a) PB and (b) PP shown for comparison to the electronic origin shifts of BHD.

helpful in making conformational assignments. The rotational band contours provided further support to these assignments.

The final conformational assignments of BHD are summarized in Figure 11 with the results of 5-phenyl-1-pentyne (PP) and 4-phenyl-1-butyne (PB) for comparison.[8] After analysis of the acetylenic and alkyl CH stretch regions, a number of pieces of evidence point consistently to the following assignments: BHD(A) to a(gg)g, BHD(B) to g(ag)a, BHD(C) to g(gg)a, BHD(D) to g(ag)g, and BHD(E) to a(ga)g. Armed with these assignments, it is worthwhile to compare the present results on BHD with the results in the preceding paper on 4-phenyl-1-butyne (PB) and 5-phenyl-1-pentyne (PP). The side chain in BHD is in some sense a composite of the butyne and pentyne side chains of these molecules.

A. The Conformation Dependence of the Electronic Frequency Shift. One issue worth returning to is the position of the $S_1 \leftarrow S_0$ origin bands. Ideally, one would like to build up a set of rules for predicting the effect of a given side chain in a particular conformation on the position of its $S_1 \leftarrow S_0$ origin band. In the present case, one wonders whether the combined shifts of the butyne and pentyne side chains can serve as a guide for predicting the positions of the bands in BHD.

In BHD, all conformers but C have one of the arms of the hexadiyne chain gauche and the other anti relative to the ring. On the basis of a comparison of the spectra of PP (Figure 11b) and BHD (Figure 11c), it appears that in such circumstances, it is the position of the pentyne chain that dominates the electronic frequency shift of the $S_1 \leftarrow S_0$ origin. Recall that the position of the pentyne chain in BHD is specified as the second and third designations in the four-letter designation for the conformers. The dotted lines in Figure 11 connect transitions from conformers with the same pentyne chain configuration. Addition of the C≡CH to the pentyne chain in the anti position with respect to the ring leads to a small red shift ($\sim$15 cm^{-1}), while addition in the gauche position produces almost no change in the transition frequency (-2 cm^{-1} for BHD(D) and $+4$ cm^{-1} for BHD(B)). Finally, the missing conformation in BHD, g(aa)g, has its pentyne chain in the anti_anti orientation, and the corresponding PP conformer is also absent in the expansion.[8]

Conformer C is the only conformer of BHD that has the two arms of the chain taking up the two gauche positions relative to the ring. This "double gauche" g(gg)a conformation produces an unusually large blue shift in the electronic frequency of the $S_1 \leftarrow S_0$ origin. One might have guessed, based on the pentyne and butyne chains by themselves, that this g(gg)a conformation would be near zero frequency shift, with the red shift of the gauche pentyne chain counteracted by a blue shift for the butyne gauche position. However, it is clear that these two groups are not merely additive but also affect one another.

The last letter in our labeling scheme denotes the relative orientation of the hexadiyne subunit. A perusal of Figure 11c indicates that all conformations with a gauche hexadiyne subunit are on the red end of the spectrum, while the two *anti*-hexadiyne configurations are to the blue. In this sense, the butyne and hexadiyne subunits are the best predictors of the ordering of the origin transitions. Using only these two labels, we see that ν[a(butyne)g(HD)] < ν[g(butyne)g(HD)] < ν[g(butyne)a(HD)].

B. The Conformation Dependence of the Transition Moment. An interesting result of this study is the observation of the restoration of the TDM orientation to the *b*-axis in conformation C. As Pratt and co-workers[15,17,29] have pointed out, in symmetric monosubstituted benzenes (i.e., phenylacetylene and *anti*-propylbenzene) the TDM lies along the *b*-axis, and there is a normal ordering of states where ^1L_b lies below ^1L_a. In substituted benzenes with off axis substituents (i.e., gauche alkylbenzenes) the TDM lies between the *a* and *b* axes (of the benzene ring). This reorientation of the TDM is attributed to the mixing of the excited-state MOs (LUMO and LUMO+1) where the new excited-state LUMO and LUMO+1 are no longer symmetric and antisymmetric, respectively, about the *a* and *b* axes. As a result the excited state is a mixture of ^1L_a and ^1L_b. CIS calculations correctly predict these results.

The BHD MOs (CIS/6-31G) involved in the $S_1 \leftarrow S_0$ transition are shown in Figure 12. As anticipated, the LUMO and LUMO+1 are distorted away from the axes parallel of perpendicular to the point of substitution in all conformations except g(gg)a. This is consistent with the observed mixed *a*/*b* TDM in all conformers except BHD(C). In conformer C

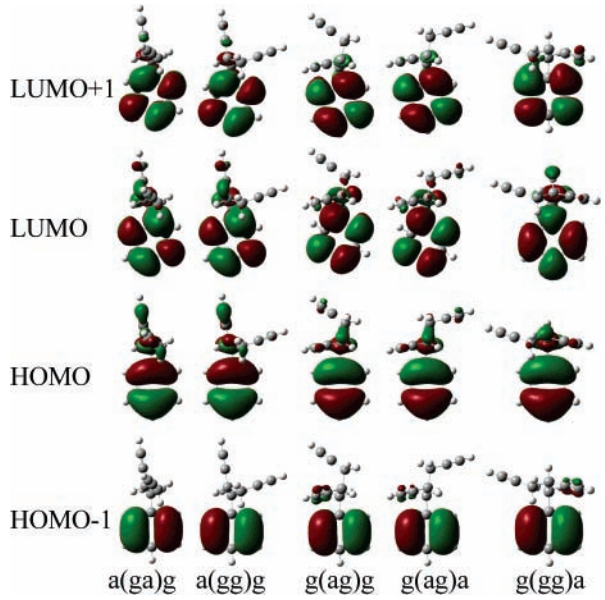

Figure 12. Molecular orbitals involved in the $\pi \rightarrow \pi^*$ transition of selected conformations of BHD.

(g(gg)a), the LUMO and LUMO+1 have their symmetry restored by the double-gauche configuration for the hexadiyne chain. This reclaims the "*b*" type character to the band in BHD-(C), as observed experimentally. Similar restoration of the *b*-axis oriented TDM by substitution of benzene with two symmetrically related "off-axis" substituents was reported in a study of the divinylbenzenes by Nguyen et al.[30]

Acknowledgment. The authors gratefully acknowledge the support of the Department of Energy Basic Energy Sciences, Division of Chemical Sciences under Grant No. DE-FG02-96ER14656.

Supporting Information Available: Text giving the synthesis of 3-benzyl-1,5-hexadiyne. This material is available free of charge via the Internet at http://pubs.acs.org.

References and Notes

(1) Tancell, P. J.; Rhead, M. M.; Pemberton, R. D.; Braven, J. *Fuel* **1996**, *75*, 717.
(2) Roubaud, A.; Lemaire, O.; Minetti, R.; Sochet, L. R. *Combust. Flame* **2000**, *123*, 561.
(3) Miller, J. A.; Klippenstein, S. J. *J. Phys. Chem. A* **2001**, *105*, 7254.
(4) Hopf, H. *Angew. Chem.* **1970**, *82*, 703.
(5) Harman, P. J.; Kent, J. E.; O'Dwyer, M. F.; Griffith, D. W. T. *J. Phys. Chem.* **1981**, *85*, 2731.
(6) Kent, J. E.; Harman, P. J.; O'Dwyer, M. F. *J. Phys. Chem.* **1981**, *85*, 2726.
(7) Asmis, K. R.; Allan, M.; Schafer, O.; Fulscher, M. *J. Phys. Chem. A* **1997**, *101*, 2089.
(8) Selby, T. M.; Zwier, T. S. *J. Phys. Chem. A* **2005**, *109*, 8487.
(9) Dian, B. C.; Clarkson, J. R.; Zwier, T. S. *Science* **2004**, *303*, 1169.
(10) Clarkson, J. R.; Dian, B. C.; Moriggi, L.; DeFusco, A.; McCarthy, V.; Jordan, K. D.; Zwier, T. S. *J. Chem. Phys.* **2005**, *122*, 214311.
(11) Clarkson, J. R.; Baquero, E.; Zwier, T. S. *J. Chem. Phys.* **2005**, *122*, 214312.
(12) Clarkson, J. R.; Baquero, E.; Shubert, V. A.; Myshakin, E.; Jordan, K. D.; Zwier, T. S. *Science* **2005**, *307*, 1443.
(13) Selby, T. M.; Clarkson, J.; Mitchell, D.; Fitzpatrick, J. A. J.; Lee, H. D.; Pratt, D. W.; Zwier, T. S. *J. Phys. Chem. A* **2005**, *109*, 4484.
(14) Dickinson, J. A.; Joireman, P. W.; Kroemer, R. T.; Robertson, E. G.; Simons, J. P. *J. Chem. Soc., Faraday Trans.* **1997**, *93*, 1467.
(15) Borst, D. R.; Joireman, P. W.; Pratt, D. W.; Robertson, E. G.; Simons, J. P. *J. Chem. Phys.* **2002**, *116*, 7057.
(16) Hopkins, J. B.; Powers, D. E.; Smalley, R. E. *J. Chem. Phys.* **1980**, *72*, 5039.
(17) Kroemer, R. T. L.; K. R; Dickinson, J. A.; Robertson, E. G.; Simons, J. P.; Borst, D. R.; Pratt, D. W. *J. Am. Chem. Soc.* **1998**, *120*, 12573.
(18) Arrington, C. A.; Ramos, C.; Robinson, A. D.; Zwier, T. S. *J. Phys. Chem. A* **1998**, *102*, 3315.
(19) Stearns, J. A.; Zwier, T. S. *J. Phys. Chem. A* **2003**, *107*, 107117.
(20) Becke, A. D. *Phys. Rev. Sect. A.* **1988**, *38*, 3098.
(21) Lee, C.; Yang, W.; Parr, R. G. *Phys. Rev. Sect. B.* **1988**, *37*, 785.
(22) Frisch, M. J.; Pople, J. A.; Binkley, J. S. *J. Chem. Phys.* **1984**, *80*, 3265.
(23) Woon, D. E.; Dunning, T. H., Jr. *J. Phys. Chem.* **1993**, *98*, 1358.
(24) Kendall, R. A.; Dunning, T. H., Jr.; Harrison, R. J. *J. Phys. Chem.* **1992**, *96*, 6796.
(25) Foresman, J. B.; Head-Gordon, M.; Pople, J. A.; Frisch, M. J. *J. Phys. Chem.* **1992**, *96*, 135.
(26) Mohamadi, F.; Richard, N. G. J.; Guida, W. C.; Liskamp, R.; Lipton, M.; Caufield, C.; Chang, G.; Hendrickson, T.; Still, W. C. *J. Comput. Chem.* **1990**, *11*, 440.
(27) Frisch, M. J. T.; G. W.; Schlegel, H. B.; Scuseria, G. E.; Robb, M. A.; Cheeseman, J. R.; Zakrzewski, V. G.; J. A. Montgomery, J.; Stratmann, R. E.; Burant, J. C.; Dapprich, S.; Millam, J. M.; Daniels, A. D.; Kudin, K. N.; Strain, M. C.; Farkas, O.; Tomasi, J.; Barone, V.; Cossi, M.; Cammi, R.; Mennucci, B.; Pomelli, C.; Adamo, C.; Clifford, S.; Ochterski, J.; Petersson, G. A.; Ayala, P. Y.; Cui, Q.; Morokuma, K.; Malick, D. K.; Rabuck, A. D.; Raghavachari, K.; Foresman, J. B.; Cioslowski, J.; Ortiz, J. V.; Baboul, A. G.; Stefanov, B. B.; G. Liu, A. L.; Piskorz, P.; Komaromi, I.; Gomperts, R.; Martin, R. L.; Fox, D. J.; Keith, T.; Al-Laham, M. A.; Peng, C. Y.; Nanayakkara, A.; Gonzalez, C.; Challacombe, M.; Gill, P. M. W.; Johnson, B.; Chen, W.; Wong, M. W.; Andres, J. L.; Gonzalez, C.; Head-Gordon, M.; Replogle, E. S.; Pople, J. A. Gaussian 98, Revision A.7. Gaussian, Inc.: Pittsburgh, PA, 1998.
(28) D. F. Plusquellic, R.; Suenram, R. D.; Mate, B.; Jensen, J. O; Samuels, A. C. *J. Chem. Phys.* **2001**, *115*, 3057.
(29) Ribblett, J. W.; Borst, D. R.; Pratt, D. W. *J. Chem. Phys.* **1999**, *111*, 8454.
(30) Nguyen, T. V.; Ribblett, J. W.; Pratt, D. W. *Chem. Phys.* **2002**, *283*, 279.